Glacier extent in sub-Antarctic Kerguelen archipelago from MIS 3 period: Evidence from 36Cl dating

Vincent Jomelli, Irene Schimmelpfennig, Vincent Favier, Fatima Mokadem, Amaelle Landais, Vincent Rinterknecht, Daniel Brunstein, Deborah Verfaillie, Claude Legentil, Georges Aumaitre, et al.

Glacier extent in sub-Antarctic Kerguelen Archipelago from MIS 3 period: Evidence from 36 Cl dating

Vincent Jomelli[1*], Irene Schimmelpfennig[2], Vincent Favier[3], Fatima Mokadem[1], Amaelle Landais[4], Vincent Rinterknecht[1], Daniel Brunstein[1-5], Deborah Verfaillie[3], Claude Legentil[1], Georges Aumaitre [2-6], Didier L. Bourlès[2-6], Karim Keddadouche[2-6].

1- Université Paris 1 Panthéon-Sorbonne, CNRS Laboratoire de Géographie Physique, 92195 Meudon, France.* corresponding author vincent.jomelli@lgp.cnrs.fr

2-Aix Marseille Univ, CNRS, IRD, Coll France, CEREGE, Aix-en-Provence, France

3- Univ. Grenoble Alpes, LGGE, Grenoble, CNRS, France.

4- Laboratoire des Sciences du Climat et de l'Environnement – IPSL, UMR8212, CEA-CNRS-UVSQ-UPS, Gif sur Yvette, France

5- Università di Corsica - Pasquale Paoli, UMR CNRS 6240 LISA, Corte, France.

6- ASTER Team.

Abstract

Documenting sub-Antarctic glacier variations during the local last glacial maximum is of major interest to better understand their sensitivity to atmospheric and oceanic temperature changes in conjunction with Antarctic ice sheet changes. However, data are sparse because evidence of earlier glacier extents is for most sub-Antarctic islands located offshore making their observation complex. Here, we present 22 cosmogenic ^{36}Cl surface exposure ages obtained from five sites at Kerguelen to document the glacial history. The ^{36}Cl ages from roche moutonnee surfaces, erratics and boulders collected on moraines span from 41.9 ± 4.4 ka to 14.3 ± 1.1 ka. Ice began to retreat on the eastern part of the main island before 41.4 ± 4.4 ka. Slow deglaciation occurred from ~41 to ~ 29 ka. There is no evidence of advances between 29 ka and the Antarctic Cold Reversal (ACR) period (~14.5-12.9 ka) period. During the ACR, however, the Bontemps and possibly Belvedere moraines were formed by the advance of a Cook Ice Cap outlet glacier and a local glacier on the Presque Ile Jeanne d'Arc, respectively. This glacier evolution differs partly from that of glaciers in New

Zealand and in Patagonia. These asynchronous glacier changes in the sub-Antarctic region are however in agreement with sea surface temperature changes recorded around Antarctica, which suggest differences in the climate evolution of the Indo-Pacific and Atlantic sectors of Antarctica.

Keywords: Glacier fluctuations, 36Cl cosmic-ray exposure dating, MIS 2-4, Kerguelen

Highlights

- Little is known about glacier fluctuations in sub-Antarctic regions.
- We present 22 cosmogenic ^{36}Cl surface exposure ages in Kerguelen Islands.
- The ^{36}Cl ages from erratic and moraine boulders span from 41 ka to 14 ka.
- Ice began to retreat on the eastern part of the main island before 41.4 ± 4.4 ka.
- Slow deglaciation occurred from ~41 to ~ 29 ka.
- This pattern of deglaciation partly differs from that of glaciers in New Zealand and in Patagonia due to different regional climate conditions.

1. Introduction

Hodgson et al (2014) published a synthesis of terrestrial and submarine evidence of the extent and timing of the global Last Glacial Maximum (gLGM 26, 500-19, 000 years ago) (Clark et al., 2009) and the onset of deglaciation on the maritime-Antarctic and sub-Antarctic islands in the framework of the Scientific Committee for Antarctic Research (SCAR). Based on the lack of glacier chronologies or indirect evidence of glacier extents from the local LGM (lLGM), Kerguelen archipelago, located in the Indian Ocean (49°S, 69°E; Fig 1), was classified as an area with a limited lLGM ice extent, but as subject to extensive earlier continental shelf glaciations. The Kerguelen archipelago is, however, the largest currently glaciated area in sub-Antarctic regions with numerous terrestrial glaciers. The Cook Ice Cap (CIC) and smaller glaciers

covered a total area of 520 km^2 in 2009 (Berthier et al., 2009). These glaciers are known to be very sensitive indicators of climate change in the southern polar region. Favier et al (2016) showed that the current high wastage of the largest CIC outlet Ampere glacier was driven by atmospheric drying, which was induced by a latitudinal shift of the storm track over the last decades. This latitudinal storm track shift is mainly driven by the Southern Annular Mode, whose positive phase (SAM+) is associated with a belt of low pressure surrounding Antarctica (Thompson and Wallace, 2000; Thompson et al., 2011). In addition, Jomelli et al (2017) provided chronological evidences of a general glacier retreat since the Late Glacial in Kerguelen and suggested that this glacier retreat was concomitant with warming and snow accumulation decrease in Antarctica, thus demonstrating the sensitivity of the CIC to climate change in the Antarctic region.

Considering this connection between glaciers in Kerguelen and Antarctic climate, new investigations on glacier extensions during and before the lLGM in Kerguelen is particularly relevant. It raises questions regarding their relative pacing with Antarctic climate and ice sheet changes. Moreover, a comparison of several ice core records from West and East Antarctic Ice Sheets revealed distinct variations, pointing to differences in the climate evolution of the Indo-Pacific and Atlantic sectors of Antarctica (Stenni et al., 2010, 2011). A better knowledge of glacier changes at Kerguelen may be relevant to discussing possible differences in glacier behavior between the Indo-Pacific and Atlantic sectors of sub-Antarctic regions.

To address these issues, a field campaign organized in the framework of two IPEV(Institut Paul Emile Victor) programs (Kesacco and Glacepreker) was conducted focusing on the geomorphology and the chronology of several glacially formed landscapes and deposits at the margin of the CIC with the aim to document the timing and extent of the LGM in Kerguelen. Here, we present 22 new ^{36}Cl cosmic-ray exposure ages obtained from roche moutonnee surfaces, erratics and boulders collected on moraines over the whole extent of the main island.

2. Study area

The French Kerguelen basaltic archipelago is located in the southern Indian Ocean (49°N, 69°E) about 2000 km north of Antarctica. It is composed of one main island with an area of 6,700 km^2 and about 300 smaller islands (Fig. 1) emerged from the Kerguelen oceanic plateau about 40 Ma ago. It stretches over a distance of about 150 km. The western part of the archipelago is covered by the CIC, the largest ice cap on this island (410 km^2 in 2011, Verfaillie et al., 2015), which is culminating at 1,030 m above sea level (a.s.l.).

Glaciers are also present at the base of three summits, at Mont Ross 1,850 m a.s.l., the highest summit on Kerguelen about 40 km south east of CIC, as well as on the highest slopes of Rallier du Bathy (1100 m a.s.l) 45 km south of CIC and on Presqu'ile de la Société de Géographie (1081 m a.s.l). The eastern part of the archipelago forms an ice free peninsula with a mean elevation of 200 m a.s.l.. However, numerous undated glacial features such as erratic boulders, kettles, and Rogen moraines demonstrate that this area was covered by ice in the past (Hall, 1984). It is probable that evidence of earlier glacier extent exists off shore. To date, a LGM frontal moraine may have been identified from bathymetry off shore from Ampere glacier (Jomelli et al., 2017).

There is only one permanent weather station on the Kerguelen Islands, located at the scientific station Port aux Français (PAF) (12 m a.s.l.) with daily values of temperature and precipitation available since 1951. Here the mean annual temperature is 4.6°C with 800 mm of precipitation. However, the precipitation amounts on the main island are affected by a strong W-E gradient due to foehn effect on the eastern side of CIC, which constitutes a barrier to the dominant westerly winds. At CIC, the precipitation amount reaches 3,150 mm per year at 250 m a.s.l. (Verfaillie et al., 2015).

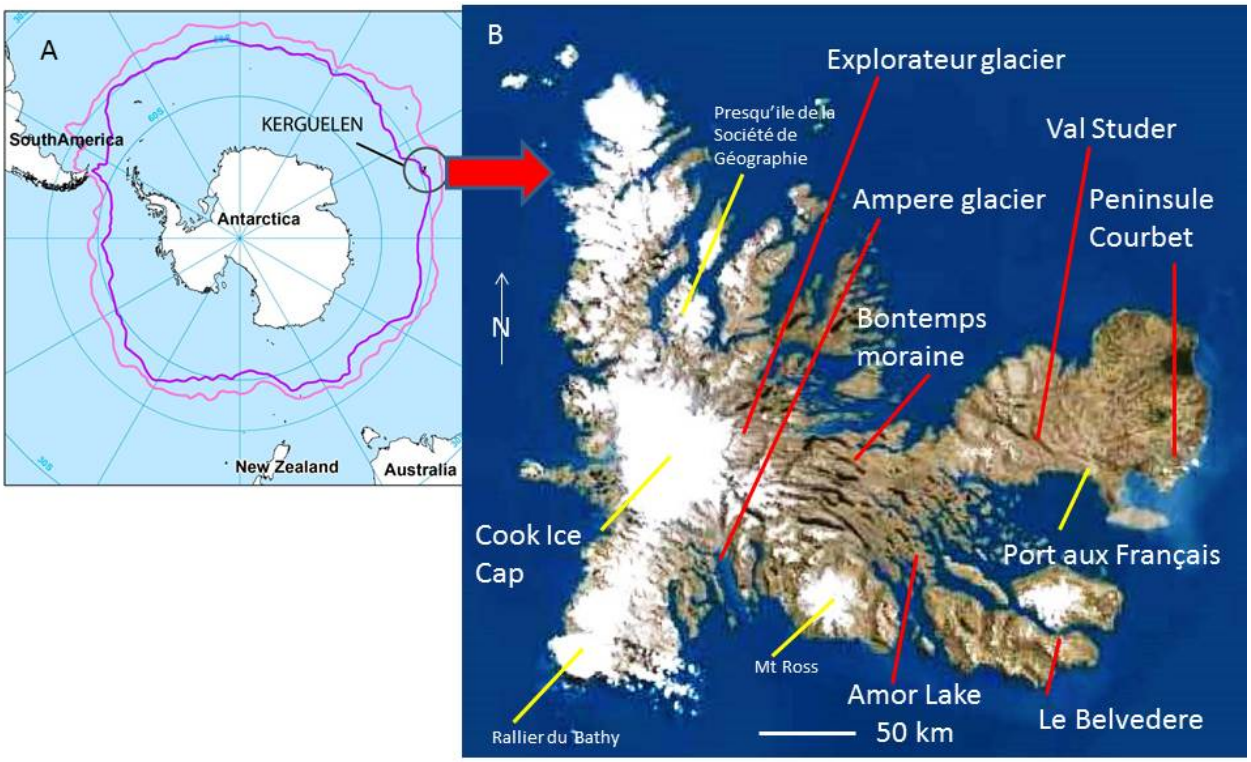

Fig. 1. General location of the study area. A. Map of the Kerguelen (black circle) and sub-Antarctic areas, with the mean positions of the sub-Antarctic (pink) and polar (purple) oceanic fronts between 1993 and 2005. B. Red lines

show the five cosmogenic sample sites investigated in this study; yellow lines show geographic locations described in the paper.

3. Previous glaciological studies on glaciers at Kerguelen

The first glaciological investigations at Kerguelen were realized in the 1970s, during which surface energy and mass balance studies (Poggi, 1977; Vallon, 1977a, 1977b, 1987) were conducted on Ampere glacier. Additionally, satellite images made it possible to assess CIC wastage over the last decades (Berthier et al., 2009; Verfaillie, et al., 2015). During the last six years, new glaciological investigations were conducted at Kerguelen. Ablation stakes were set up in December 2010 and January 2011 and were measured during the next three years to assess the glacier surface mass balance. A total loss of 1.6 meter water equivalent per year (m w.e. a^{-1}) was measured over the ice cap between 1960 and 2011, with a maximum loss of 2.76 m w.e. a^{-1} on Ampere glacier. From a detection attribution analysis, Favier et al. (2016) demonstrated that precipitation decrease was the first order cause for glacier wastage since the 1960s. Precipitation changes were attributed to a shift of the latitudinal position of the storm track mainly driven by the Southern Annular Mode (SAM) whose positive phase (SAM+) is associated with a belt of low pressure surrounding Antarctica (Thompson and Wallace, 2000; Thompson et al., 2011) and dry conditions at Kerguelen.

To better understand the long term evolution of glaciers at Kerguelen, 13 cosmogenic ^{36}Cl surface exposure ages were determined at four sites, one located close to Ampere glacier front position and three 20 km away from the CIC (Jomelli et al., 2017). These data were combined with existing radiocarbon ages from terrestrial and marine sediments cores, bathymetric measurements and a relative dating technique that uses the radial growth of *Azorella selago* Hook, a cushion-forming Umbelliferae species growing on the moraine (Frenot et al 1993; 1997). Results revealed that deglaciation started at least ~24 ka ago and that the landscape up to 20 km east of CIC was still partly covered by ice during the Late glacial. Glaciers were shrinking through the Holocene probably until 3 ka with evidence of minor advances during the last millennium (Jomelli et al., 2017).

4. Methods

The fieldwork was conducted in different areas of the Kerguelen Islands on the slope east of the CIC in order to complement a previous study (Jomelli et al., 2017) and document earlier glacier extents on the main Island at various altitudes and distances from CIC. Frontal moraines are rare on the main island but erratics and roche moutonnees are very frequent making possible to document past ice extents. Five sites, Peninsule

Courbet, Val Studer, Armor Lake, Bontemps valley and Le Belvedere moraine (sample locations in Fig.1 and Table 1; note that Armor Lake and Ampere glacier were studies by Jomelli et al., 2017. Their chronologies are discussed at the end of this paper) were visited in order to collect rock samples from glacial moraine boulders, erratic boulders and roche moutonnee surfaces:

Samples were taken with a hammer and a chisel from preferentially flat surfaces of erratic and moraine boulders and of roche moutonnee. The geographic coordinates were recorded with a handheld GPS device and topographic shielding was measured using a clinometer (Table 1). The altitudes were later determined from shuttle radar topography mission data (SRTM), because they are more accurate than the handheld GPS data (Table 1).

The *in situ* ^{36}Cl dating was conducted on the basaltic whole rock samples at CEREGE, Aix-en-Provence, France, similar to the method described in Schimmelpfennig et al. (2011). An aliquot of bulk rock was taken from several samples for major and trace element analysis at the Service d'Analyse des Roches et des Minéraux (SARM, Nancy, France) (Tables 2-3), necessary to estimate the low-energy neutron flux in the samples, which induces the ^{36}Cl production from capture of the low-energy neutrons on ^{35}Cl. Due to low Cl concentrations (Table 4), this production reaction contributed little to the total ^{36}Cl production in most samples (between ~2% and ~9%), except for sample Ker-16 (16%).

After crushing and sieving to a grain size fraction of 250-500 μm, the samples were decontaminated from potentially Cl-rich groundmass and atmospheric ^{36}Cl in a diluted suprapur HF/HNO_3 acid mixture (Schimmelpfennig et al., 2009). Following this step, which removed about 40% of the initial samples weight, 2 g aliquots of the rinsed and dried sample grains were taken for analysis of the major elements concentrations by ICP-OES at SARM (Table 3), because Ca, K, Ti and Fe, are the target elements for spallogenic/muogenic production of ^{36}Cl. After addition of a ^{35}Cl-enriched spike (~99%) for isotope dilution (Ivy-Ochs et al., 2004), the samples were totally dissolved in a HF/HNO_3 acid mixture. Two chemistry blanks were processed together with the samples (Table 4). The remaining steps were identical with those described in Schimmelpfennig et al. (2011). Measurement of the ^{36}Cl/^{35}Cl and ^{35}Cl/^{37}Cl ratios by isotope dilution accelerator mass spectrometry at the AMS facility ASTER-CEREGE allowed the calculation of the ^{36}Cl and Cl concentrations (Table 4).

^{36}Cl age calculations were done using the Excel® spreadsheet published by Schimmelpfennig et al. (2009), using scaling factors based on the time-invariant "St" method (Stone, 2000) (Table 4) and applying the following ^{36}Cl production rates, referenced to sea level and high latitude (SLHL): 42.2 ± 4.8 atoms ^{36}Cl (g Ca)$^{-1}$ yr^{-1} for spallation of Ca (Schimmelpfennig et al., 2011), 148.1 ± 7.8 atoms ^{36}Cl (g K)$^{-1}$ yr^{-1} for spallation

of K (Schimmelpfennig et al., 2014), 13 ± 3 atoms ^{36}Cl (g Ti)$^{-1}$ yr^{-1} for spallation of Ti (Fink et al., 2000), 1.9 ± 0.2 atoms ^{36}Cl (g Fe)$^{-1}$ yr^{-1} for spallation of Fe (Stone et al., 2005), and 626 neutrons (g air)$^{-1}$ yr^{-1} for the production rate of epithermal neutrons from fast neutrons in the atmosphere at the land/atmosphere interface (Phillips et al., 2001). A high-energy neutron attenuation length of 160 g cm^{-2} was used. We assumed bulk rock density of 2.4 g cm^{-3} for all samples. Further relevant input data (sample thicknesses, shielding factors, compositional data) are shown in Tables 1, 2 and 3.

In Table 4, we present the 1σ uncertainties of the resulting individual ^{36}Cl ages inferred through full propagation of all errors (analytical and production rate errors) as well as of the analytical errors only. In the main text, we report the individual ages with their analytic uncertainties only for the sake of internal comparison between the ages; when presenting the mean of an age population, we report the arithmetic mean and the full error including the production rate error to allow comparison with climate records that were dated with different methods. We determined this full error by computing the standard deviation and adding analytical and production rate errors (represented by the mean of the relative individual age uncertainties) by propagation in quadrature. On the maps, all ages are shown with the full errors, unless otherwise stated. A Chi^2 test was applied to identify potential outliers within an age population.

The ^{36}Cl ages are presented without erosion or snow cover corrections. Concerning erosion, quantitative information at Kerguelen is not available at present, but during sampling, surfaces with little evidence of erosion were preferentially targeted (degree of weathering and direct evidence on the boulder surface of frost, salt or wind action). Assuming an erosion rate of 5 mm ka would result in a 10% increase of the oldest ^{36}Cl ages (erratic boulders at Peninsule Courbet) and less for the younger ages. This is within the overall uncertainties of the final ^{36}Cl ages and taking it into consideration would not change the conclusions of this study. Potential snow cover effects were not considered in the ^{36}Cl age calculations, because of the modern short annual snow cover duration (~1.5 months at 90 m altitude and ~3 weeks at 35 m altitude as inferred from glaciological modelling (Verfaillie et al., 2015; Favier et al., 2016)), which would lead to an insignificant snow cover correction.

5. Results

5.1 Erratic boulders deposited far east of CIC

208 The ^{36}Cl ages range from ~42 to ~11 ka (Table 1-4) with an ~80% contribution covering the 42-20 ka period.
209 Our dataset can be divided into three groups (erratics, roche moutonnees and moraine landforms) in terms
210 of sampled glacial features and distance from CIC.

211 The first group is composed of the 13 distant erratic boulders located at Peninsule Courbet and Val Studer.
212 Peninsule Courbet is the farthest sampling site located about 85 km east of CIC in our study, at an altitude
213 between 37 m and 57 m a.s.l. (Figs.1, 2, 3; table 1). Most of this peninsula is relatively flat with altitudes
214 lower than 100 m a.s.l. Numerous kettle lakes are visible. They are associated with losely-spaced ridges or
215 small hills 2-5 m high, mostly covered by sand and gravel with few larger boulders that may correspond to
216 a glacial till. These ridges may correspond to remains of Rogen moraines formed transverse to ice flow in a
217 subglacial position and indicating the presence of an ice sheet flowing eastward. Three samples (Ker 26,
218 Ker 27, Ker 28) were collected from large erratic boulders 8 km north east of PAF (Fig.2). These three
219 erratic are the oldest dated samples in this study. Positioned on a rocky pavement, they yield consistent ^{36}Cl
220 ages of 40.9 ± 2.7 ka, 41.9 ± 2.8 ka and 41.3 ± 2.8 ka, with a mean age of 41.4 ± 4.4 ka (Figs. 2-4, 13).

221 Erratic are rare closer the coast and on northeastern direction. Nevertheless two additional samples (Ker 29
222 and Ker 30) were collected from erratics partly embedded in a sandy gravel pavement 5 and 11 km north
223 east from the previous sampling site, respectively (Fig.2). They yield ages of 30.7 ± 2.0 ka and 26.7 ± 3.0
224 ka.

225

Fig. 2. Location of ^{36}Cl ages with their arithmetic mean at Peninsule Courbet site. The 1σ uncertainties in the individual ^{36}Cl errattic ages account for analytical and production rate uncertainties, while the uncertainty in the mean includes standard deviation, analytical and production rate uncertainties. The samples in italic were rejected as outliers based on a Chi^2 test (see text for details).

According to the Chi^2 test, these ages do not belong to the same age population as the other three dates, but are statistically indistinguishable from each other with a mean of 28.7 ± 4.3 ka. Two explanations are possible: either these two younger boulders were deposited following a later ice advance compared to the deposition of the ~41 ka boulders, or they reflect post depositional erosion or exhumation processes. Since there is no firm evidence supporting either of the two scenarios, we assume these two younger boulder ages as outliers (reflecting possible post depositional erosion or exhumation processes) and do not further consider them.

Figure 3.Pictures of some of the sites sampled during the field campaigns. A: erratic boulders Ker-28 at Peninsule Courbet. B: erratic boulders Ker-34 at Val Studer. C: sampling of the roche moutonnee near Armor Lake. D: erratic boulder Ker-38 at Val Studer.

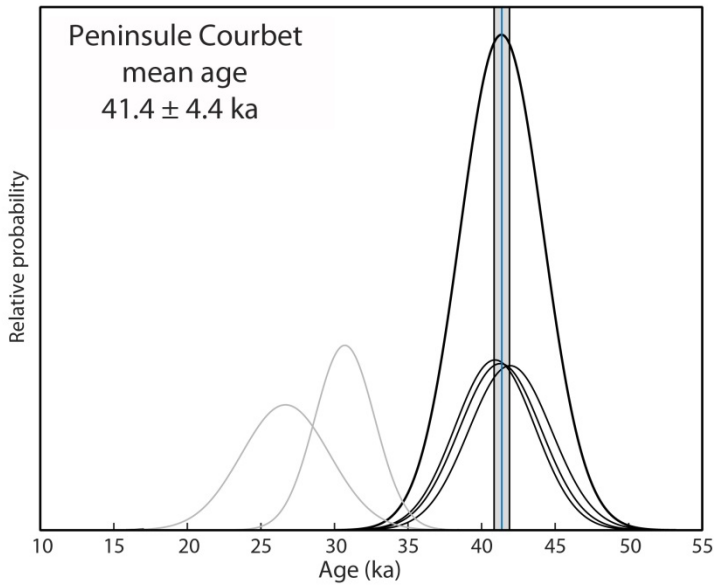

Fig 4. Probability plots of ^{36}Cl boulder ages from Peninsule Courbet. Please note that the gaussian curves of the individual ages do not include the ^{36}Cl production rate uncertainties (analytical uncertainties only), while the error of the mean age in the upper left corner box includes the ^{36}Cl production rate uncertainties. Grey curves are outliers. Vertical blue line and grey band represent arithmetic mean and standard deviation, respectively (outliers are not included).

The second sample site is Val Studer, a typical deep U-shaped glacial valley located at 60 km from CIC and about 16 km from PAF. Three erratic boulders were collected at about 320 m a.s.l. on the southern slope of Montagne Verte (716 m a.s.l.), the highest summit on the left side of Riviere du Sud. These erratics (Ker 31, 32, and 34) sampled on flat surfaces yield ^{36}Cl ages of 11.06 ± 0.86 ka, 26.5 ± 1.8 ka, and 30.8 ± 2.1 ka respectively. Rejecting Ker 31 (11.06 ± 0.86 ka) as an outlier based on the Chi^2 test, Ker 32 and Ker 34 give a mean age of 28.6 ± 4.1 ka.

About 8 km downslope five other erratic boulders were sampled on the Plateau des Drumlins between 48 and 63 m a.s.l. (Table 1, Fig. 3, 5). These boulders (Ker 35-39) yield ^{36}Cl ages of 40.6 ± 2.7 ka, 24.4 ± 1.7 ka, 38.9 ± 2.7 ka, 31.3 ± 2.1 ka and 27.8 ± 1.9 ka (Fig. 5, 6). All these boulders were also collected on flat surfaces in order to avoid downslope movements.

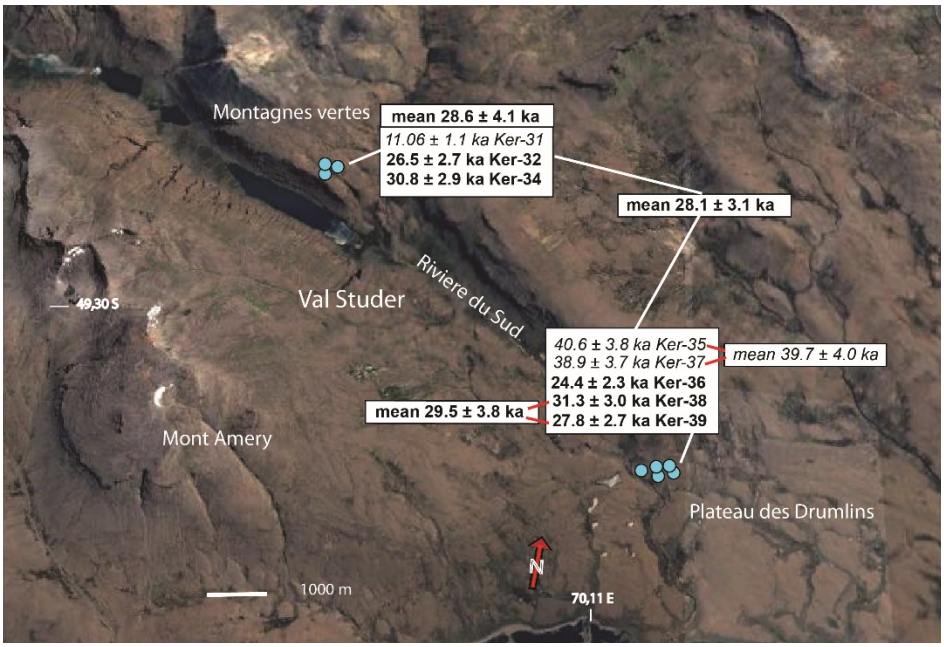

Fig. 5. Location of ^{36}Cl ages with their arithmetic means at Val Studer site. The 1σ uncertainties in the individual ^{36}Cl boulder ages account for analytical and production rate uncertainties, while the uncertainties in the means include standard deviation, analytical and production rate uncertainties. A sample in italic from Montagne Vertes was rejected as outlier based on the Chi^2 test (see text for details). For the boulders near Plateau des Drumlins there are two possible groups of outliers; see text for clarification.

Based on the Chi^2 test, two sub groups can be distinguished among samples Ker 35-39, leading us to consider two distinct hypotheses for these low elevation samples. The first hypothesis rejects the three samples Ker 35 (40.6 ± 2.7 ka), Ker 36 (24.4 ± 1.7 ka) and Ker 37 (38.9 ± 2.7 ka) as outliers. Then Ker 38 and Ker 39 yield a mean age of 29.5 ± 3.8 ka (Fig.5). This hypothesis implies a synchronous boulder deposition at the two elevations in Val Studer valley (Ker 32, Ker 34). The second hypothesis rejects the three samples Ker 36 (24.4 ± 1.7 ka), Ker 38 (31.3 ± 2.1 ka), and Ker 39 (27.8 ± 1.9 ka) as outliers. Then Ker 35 and Ker 37 yield a mean age of 39.7 ± 1.2 ka (standard deviation only) and 39.7 ± 4.0 ka (full uncertainty) (Figs. 5, 6, 13). This second hypothesis implies two distinct depositional periods at Val Studer first at Plateau des Drumlins, then at Montagnes Vertes. It also implies temporal synchronicity with the boulder ages from Peninsule Courbet, even supporting two synchronous deposition periods at both sites at ~40 ka and ~29 ka. However, this second hypothesis is not further discussed due to the lack of evidence of two boulder deposition periods. Nevertheless, this scenario does not contradict the general conclusions of this study.

Finally, considering all ages from the two altitudes in Val Studer valley (Montagnes Vertes and Plateau des Drumlins), after rejection of Ker 31, Ker 35 and Ker 37 as outliers, yields a mean age of 28.1 ± 3.1 ka (Figs.5, 6). As this mean value is not statistically different from the first hypothesis presented above (29.5

± 3.8 ka) based on the mean of the two Ker 38-39 samples but based on a larger number of boulders, it will be considered as representative for the Val Studer site in the following text.

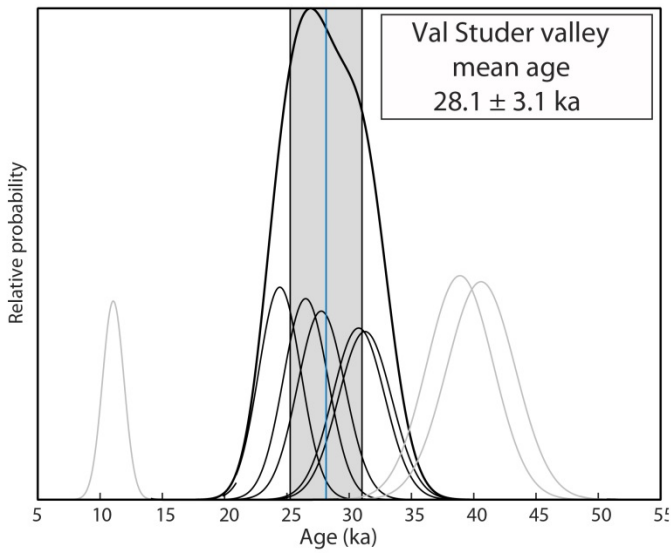

Fig 6. Probability plots of ^{36}Cl boulder ages from Val Studer. See caption of Fig. 4 for details.

5.2 Roches moutonnees at 37 km from CIC

The second group of samples comes from five roche moutonnees. Roughly 37 km east of CIC, five samples (Ker, 12, 13, 14, 15 and 16) were collected on the basaltic plateau on the south-western side of Armor Lake. Ker 12, 13 and 14 were sampled at an altitude of 132 m a.s.l and Ker 15 and 16 at 125 m a.s.l. and 53 m a.s.l. respectively (Table 1, Figs.3, 7). These roche moutonnees samples complement two ^{36}Cl ages obtained from erratic boulders located at 176 m and 177 m a.s.l. and dated to a mean age of 24.4 ± 1.1 ka (Jomelli et al., 2017).

The samples Ker 12-16 yield ^{36}Cl ages of 29.5 ± 2.1 ka, 32.1 ± 2.2 ka, 41.4 ± 2.8 ka, 30.1 ± 2.1 ka and 25.9 ± 2.0 ka respectively (Figs. 7, 8). Rejecting Ker 14 (41.4 ± 2.8 ka) as an outlier based on the Chi^2 test, the other samples yield a mean age of 29.4 ± 3.3 ka (full uncertainty). Grouping the ages previously dated by Jomelli et al., (2017) with those of the roches moutonnes and rejecting Ker 14 (41.4 ± 2.8 ka) and Ker 13 (32.1 ± 2.2 ka) as outliers, yields a mean age of 26.9 ± 3.0 ka.

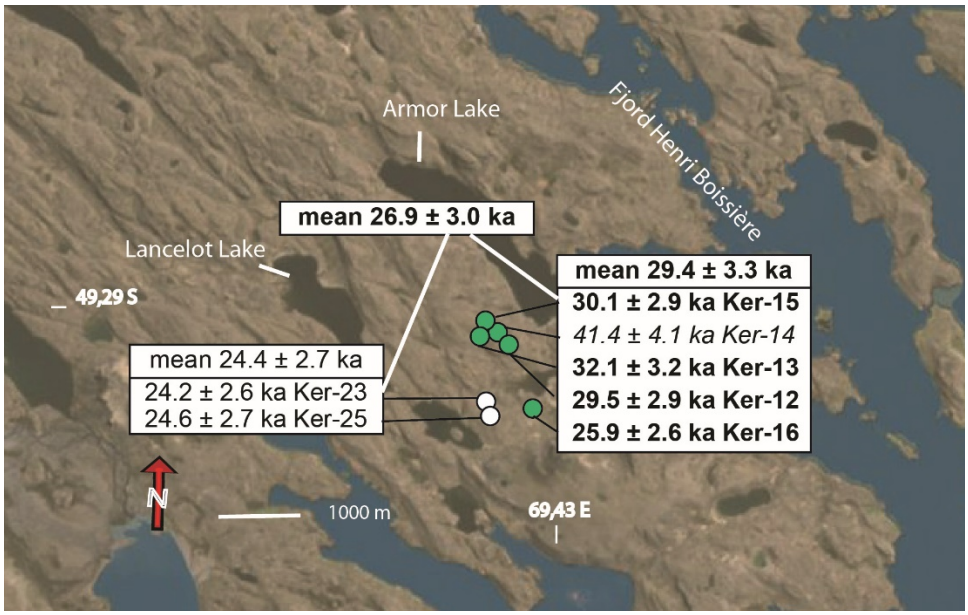

Fig. 7. Location of ^{36}Cl ages at Amor lake site. Green circles show samples from roche moutonnees with their arithmetic mean and white circles show erratic boulder ages from Jomelli et al., (2017). The 1σ uncertainties in the individual ^{36}Cl boulder ages account for analytical and production rate uncertainties, while the uncertainties in the means includes standard deviation, analytical and production rate uncertainties. The sample in italic was rejected as an outlier based on the Chi^2 test (see text for details).

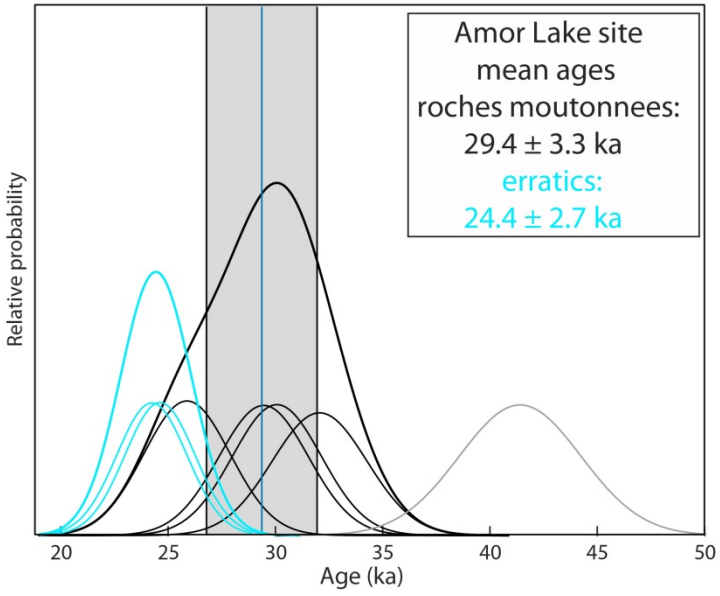

Fig. 8. Probability plots of ^{36}Cl boulder ages from Amor Lake. See caption of Fig. 4 for details. Light blue curves show ages of erratics from Jomelli et al. (2017).

5.3 Moraine landforms

The last group of ^{36}Cl ages presented in this paper is composed of four boulders on the top of two distinct moraines.

In Bontemps valley, the CIC outlet Explorateur glacier formed a prominent moraine located about 26 km down-valley from the current ice front, where it dammed Bontemps Lake, the largest lake on the main island. This moraine, covered by sub-angular large boulders (>50 cm in length), was tentatively dated to the ACR chronozone (13.3 ± 1.4 ka) by Jomelli et al (2017), based on three boulder ages, one of which was rejected as an outlier. In this study, one additional sample (KBT7) was collected from the top of this frontal moraine at 16 m a.s.l (Figs.3, 9) to better constrain the age of this moraine.

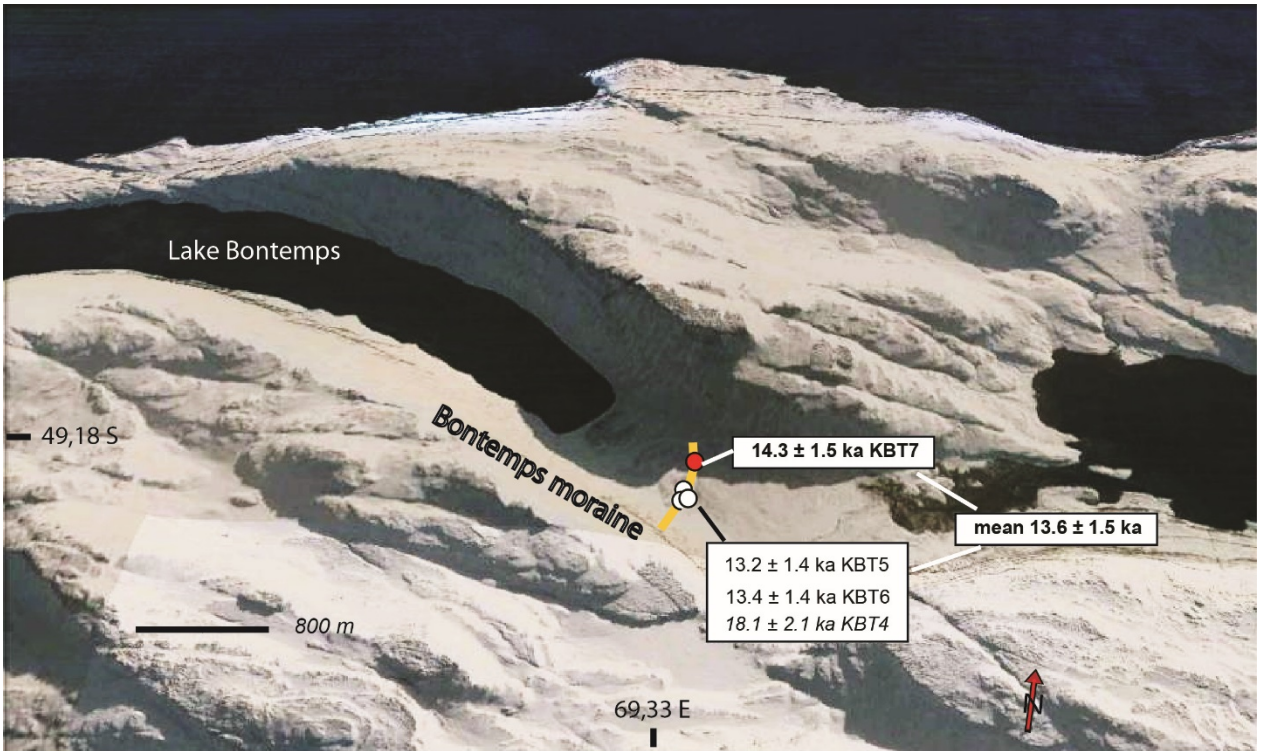

Fig.9. Sample locations in Bontemps valley with the corresponding individual ^{36}Cl ages. A red circle shows the new sample on Bontemps moraine highlighted by the yellow line, white circles show boulder ages from Jomelli et al., (2017). Also shown are the arithmetic means for the age population with the 1σ uncertainty including standard

deviation, analytical and production rate uncertainties. The sample in italic was rejected as an outlier based on the Chi^2 test (see text for details).

KBT7 is dated to 14.3 ± 1.1 ka and is consistent with previous boulder ages from the same moraine KBT5 13.2 ± 1.0 ka and KBT6 13.4 ± 1.1 ka (standard deviation only) (Fig. 9, 10, 13). All three samples from Bontemps moraine yield a mean age of 13.6 ± 1.5 ka.

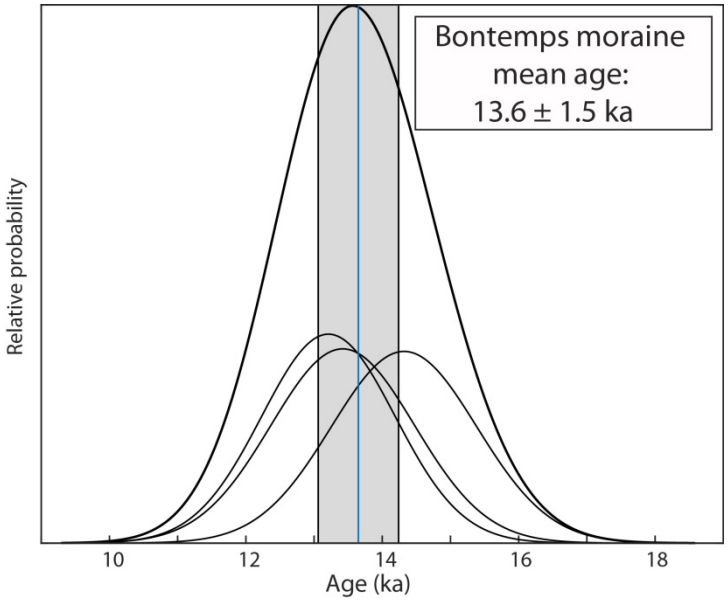

Fig. 10. Probability plots of ^{36}Cl moraine boulder ages from Bontemps moraine. See caption of Fig. 4 for details.

Three other samples HBN2, HBN3 and HBN4 were collected at an altitude between 115 and 138 m a.s.l. from boulders of about 70-100 cm height on the crest of the Belvedere moraine, about 72 km from CIC, on the southeastern part of Kerguelen about 32 km south of PAF (Fig. 11). This left lateral moraine, formed by a local glacier is located on the southern slope of a small glacial cirque below the plateau les Haut de Hurlevent. This moraine of about 300 m long and 20 m high, has steep slopes and is covered by subangular boulders.

The three samples yield ^{36}Cl ages of 15.1 ± 1.1 ka and 15.9 ± 1.3 ka and 23.8 ± 1.6 ka, respectively. From this dataset, sample HBN4 (23.8 ± 1.6 ka) was rejected as an outlier based on the Chi^2 test. This moraine boulder likely was pre-exposed to cosmic radiation and reworked during the last glacier advance. The remaining two consistent moraine boulder ages yield a mean of 15.5 ± 1.8 ka (Figs. 3, 11, 12).

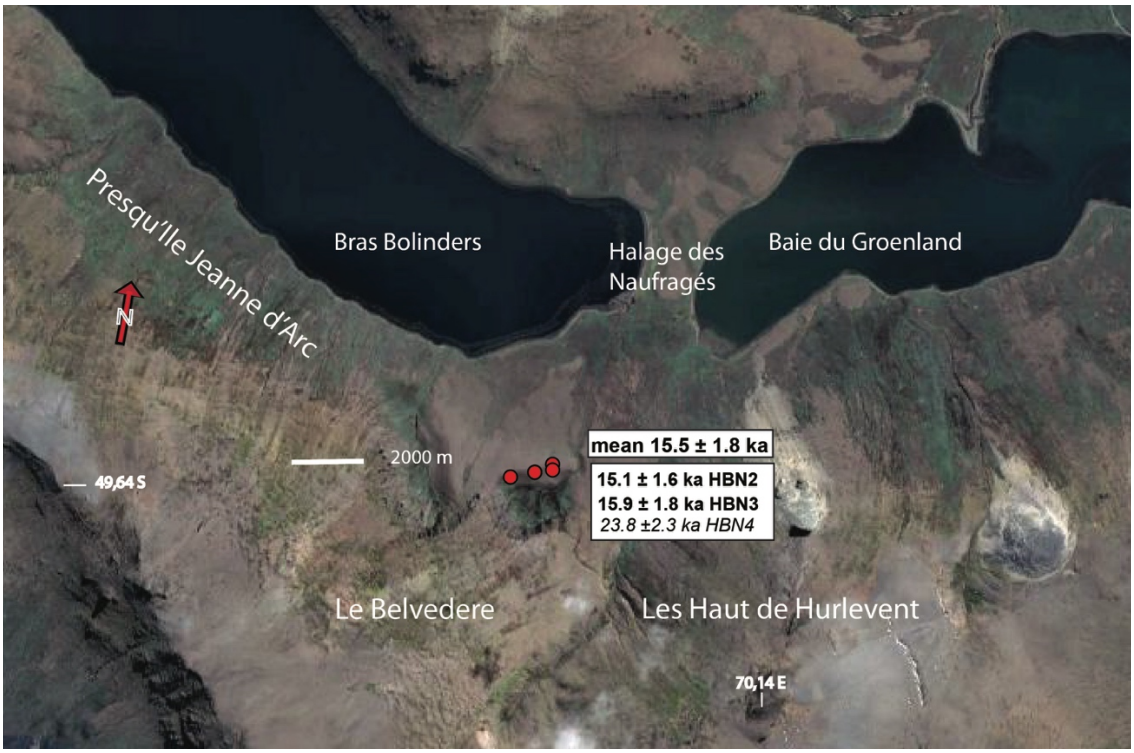

385

386 Fig. 11. Location of ^{36}Cl ages on Belvedere moraine site. The 1σ uncertainties in the individual ^{36}Cl boulder ages
387 account for analytical and production rate uncertainties, while the uncertainty in the mean includes standard deviation,
388 analytical and production rate uncertainties. The sample in italic was rejected as an outlier based on the Chi^2 test (see
389 text for details).

390

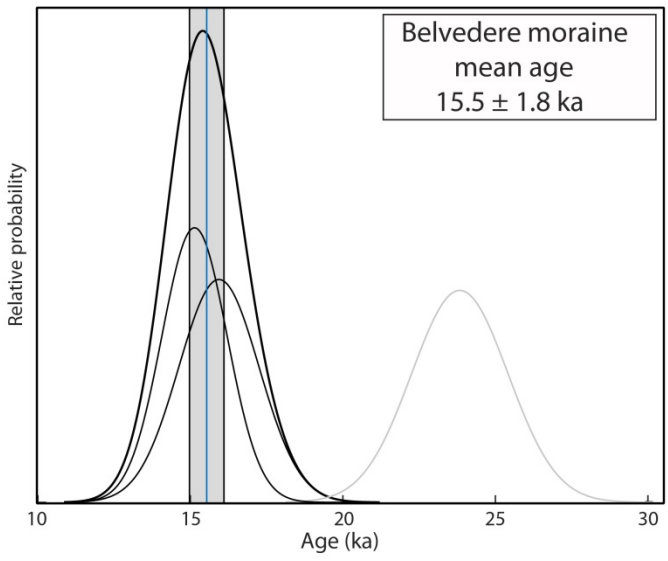

391

392 Fig. 12. Probability plots of ^{36}Cl boulder ages from Belvedere moraine. See caption of Fig. 4 for details.

6. Discussion

6.1 History of glacier fluctuations at Kerguelen from 41 ka to the late glacial

^{36}Cl cosmic-ray exposure dating of glacial erratics, roches moutonnees and morainic boulders collected at different sites over Kerguelen archipelago provide constraints on the glacier extents on the island from 41 ka to the late glacial period. Erratics from Peninsule Courbet, the farthest site east of CIC provide direct evidence that this part of the main island of Kerguelen was deglaciated ~41 ka ago (Fig. 13). These erratics most likely do not represent the maximum glacier position and were probably transported by the ice during a glacier advance that pre-dates ~41 ka ago.

Over the time period lasting from ~41 to ~29 ka, glacier shrinkage generally continued, possibly interrupted by stagnation or minor advances. We assume that before ~ 29 ka, outlet glaciers of CIC (or the glaciers that developed locally) had not retreated beyond the sample sites of Armor Lake and Val Studer for a significant period of time. This is supported by the similarity of the ages of the roches moutonnees at Armor Lake (~29 ka) and those of the erratic boulder at Val Studer (~28 ka). If the glaciers had retreated further for a significant period of time, the exposure duration of the roches moutonnees would have been longer than that of the erratics. Moreover, the age of the erratics at Armor Lake (~24 ka) suggests that after ~29 ka the ice might have retreated to an unknown position for at most ~5 ka before readvancing at ~24 ka. In addition, the uncertainties associated with the ages at Val Studer and Armor Lake do not allow us to reach a resolution good enough to highlight possible (a)-synchronies of the CIC outlet glacier fluctuations in this part of the archipelago.

After ~24 ka, the CIC outlet glaciers continued to retreat likely until the Antarctic Cold Reversal (ACR) period (14.5-12.9 ka). During this ACR period the Explorateur glacier, a CIC outlet, stagnated or re-advanced forming, 26 km from its current front position the Bontemps moraine at about 13.6 ± 1.5 ka ago. The local glacier located on the Presqu Ile Jeanne d'Arc formed the Belvedere moraine at about 15.5 ± 1.8 ka ago, which might have been contemporaneous with the formation of Bontemps moraine given their overlapping age uncertainties.

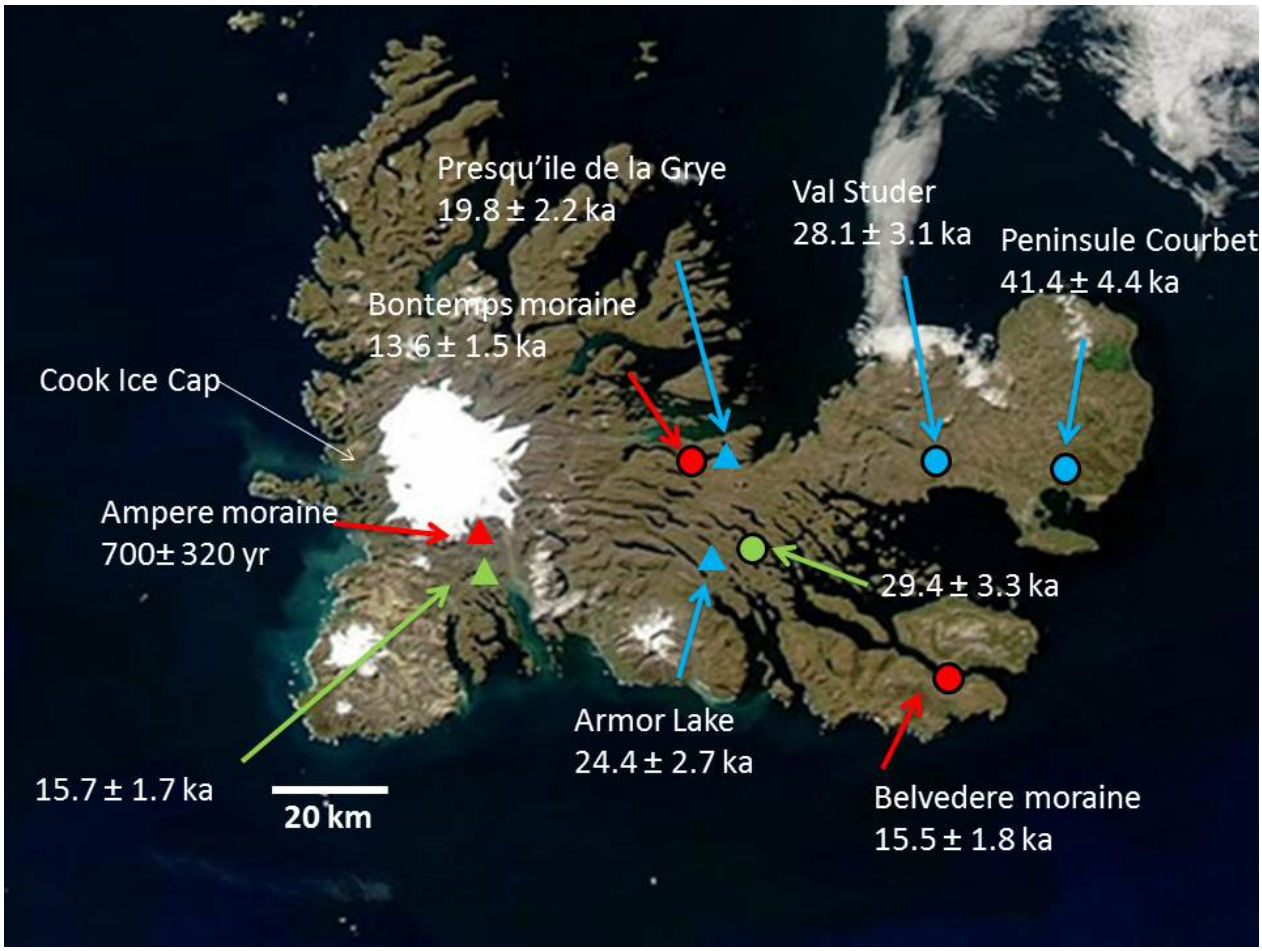

Fig. 13. Summary of ^{36}Cl ages obtained at different sample sites. Reported mean ^{36}Cl boulder ages account for standard deviation, analytical and production rate uncertainties. Red = moraine ages; Blue = erratic ages; Green = roche moutonnee age; dot = this paper; triangle = ages from Jomelli et al (2017) only.

6.2 Comparison to other sub-Antarctic glacial chronologies

Comparing our findings from the southern Indian Ocean with other sub-Antarctic glacial chronologies located in the South Pacific (New Zealand) and South Atlantic regions (Patagonia) reveals intriguing features (Fig. 14). The presented cosmic-ray exposure ages indicate that glacier retreat occurred in Kerguelen roughly 41 ka ago with a preceding glacier advance that must have been larger than that during the gLGM. Unfortunately, the exact location of the corresponding maximum CIC front position is unknown, as it might be offshore. The exact age of the glacier maximum extent that precedes the subsequent retreat

around 41 ka ago remains therefore also unknown. These findings do not fully correspond to what is documented in the two other regions.

The glacier evolution at Kerguelen only partly resembles that described in New Zealand. Kelley et al., (2014) showed that Pukaki and Mt John glaciers in New Zealand started to retreat from a major extent about 42 ka ago based on ^{10}Be ages. At Pukaki, the glacier extent during the maximum MIS-3 ice cover was comparable to the subsequent glacier culminations, which occurred between 28 ka and 25 ka, as well as 21 ka and 18 ka ago (Kelley et al., 2014). Consequently, in both regions, glaciers were larger during the MIS-3 period than during the gLGM. At Kerguelen, large glacier extent occurred 42 ka ago, but it does not necessarily correspond to a maximum glacial advance. In both regions, comparable subsequent glacier extents occurred between about 28 ka and 19 ka ago, even if field evidence of a clear glacier advance at Kerguelen at 25, 21 and 18 ka ago are still lacking. Moreover, observations covering the more recent periods revealed significant differences in glacier evolution between the two regions (Schaefer et al., 2015; Jomelli et al 2017).

Glacier evolution at Kerguelen also differs partly from Patagonia. In Patagonia, there is no clear evidence of large advances at 42 ka (Darvill et al., 2015). Fogwill et al. (2015) showed in a compilation of 59 cosmogenic ages (^{10}Be and ^{36}Cl ages) that the culmination of the ice sheet during the lLGM occurred about 28 ka ago, i.e. few millennia before the gLGM. However, this lLGM extent was smaller than pre lLGM glacier MIS-3 extents that mostly occurred at roughly 32 ka about 49°S (same latitude as Kerguelen) as well as at higher latitudes (Darvill et al., 2015). Uncertainties associated with the ^{36}Cl ages do not permit to assess synchronous advances with those documented in Patagonia between 32 and 28 ka ago. In addition, field evidence of a clear glacier advance at Kerguelen around 32 ka ago is still lacking. Also, glacier retreat in Patagonia between 28 ka to 19 ka ago was larger than at Kerguelen. These different patterns of glacier fluctuations in sub-Antarctic regions raise questions about the potential drivers of the glacier fluctuations in the southern hemisphere.

Several hypotheses have been proposed to explain the major glacier advance during the MIS-3 period but a full understanding of the forcings involved in the glacier evolution at the hemispheric scale remains puzzling (Putnam et al., 2013; Kelley et al., 2014; Darvill et al., 2015; Schaefer et al., 2015).

It is generally assumed as inferred from proxy data, that a northward migration and intensification of the southern westerly wind belt occurs during colder periods in Antarctica resulting in reduced deep ocean ventilation and low atmospheric CO_2 concentrations (Lamy et al., 2010; Fletcher and Moreno, 2011). On the other hand, model studies show contrasting results on the position and strength of the westerly winds

during the LGM conditions with either an equatorward or a poleward position (Otto Bliesner et al., 2006; Rojas et al., 2009; Sime et al., 2013).

Numerous ice core records have been extracted from the west and east Antarctic ice sheets (e.g. Watanabe et al., 2003; EPICA comm members, 2004, 2006; Stenni et al., 2011; Wais Divide, 2015). Every site temperature reconstructions based on $\delta^{18}O$ of ice cores show a progressive cooler trend during MIS-3 period with a major temperature minimum between 28 and 22 ka corresponding to the gLGM (Stenni et al., 2010; Parrenin et al., 2013; Wais Divide, 2015). These observations are the same in both the Indo-Pacific and the Atlantic sectors. Temperature and snow accumulation changes documented at Wais Divide showed a remarkable concordance with glacier changes at Kerguelen over the last 28 ka (Jomelli et al., 2017). However warm temperature in Antarctica during the pre-gLGM is counterintuitive with large glacier extent at that time observed in different regions of mid southern hemisphere. This suggests an important regional variability during the pre-LGM period. This regional variability is also seen in Antarctic ice core records over Marine Isotopic Stage 3 (MIS 3, 60 to 25 ka) during the succession of Antarctic Isotopic Maxima (AIM) associated with the abrupt Dansgaard-Oeschger events in Greenland. The warming phases of the AIM show strong variability when comparing the Atlantic and Indian-Pacific basins: it is much more rapid (a few centuries) on the Atlantic side. This creates a transient climatic dipole during warming phase of the AIMs with the Atlantic side of Antarctica being warmer than the Indian-Pacific side.

Interestingly, several sea surface temperature (SST) reconstructions have been produced making possible the documentation of climate conditions in the Indian, Pacific and Atlantic circum-Antarctic regions (Pahnke and Sachs, 2006; Kaiser and Lamy, 2010). These SSTs point to significant differences in the climate evolution of the Indo-Pacific and Atlantic sectors over the last 60 ka (Fig.14). Sub-Antarctic SSTs from N Chatham Rise MD97-2120 sediment core located south east of New Zealand (45°S) show a long period lasting from 48 ka and 28 ka ago with relatively cold conditions (Pahnke and Sachs, 2006). Minima coincide with large glacier extent. On the north west of Kerguelen, SSTs from Cape Basin 1089/TN057 sediment core (41°S) show a different pattern with a progressive warming trend from a minimum 43 ka ago, interrupted by periodic cold peaks (Pahnke and Sachs, 2006). On the east coast of Patagonia, SSTs from the sediment core ODP Site 1233 (41°S) reveal several cold episodes, in particular at 43 ka, 32 ka and 22 ka (Kaiser and Lamy, 2010). A parallel can be drawn between these differences in regional SSTs conditions and reconstructions of surface air temperature or climate of the evaporative source regions from proxy data in various Antarctic ice core records. Indeed and as mentioned above for the surface air temperature reconstruction from water isotopes, water isotopic records ($\delta^{18}O$ and d-excess) show strong differences during AIM warming phases between ice cores located on the Atlantic side of Antarctica and ice cores

located on the Indian – Pacific sides of Antarctica (Stenni et al., 2010; Buiron et al., 2012; Landais et al., 2015). At Kerguelen uncertainties associated with the ^{36}Cl ages do not permit to assess synchrony between glacier changes and AIMs but we notice that nine AIMs occurred during MIS 3 period.

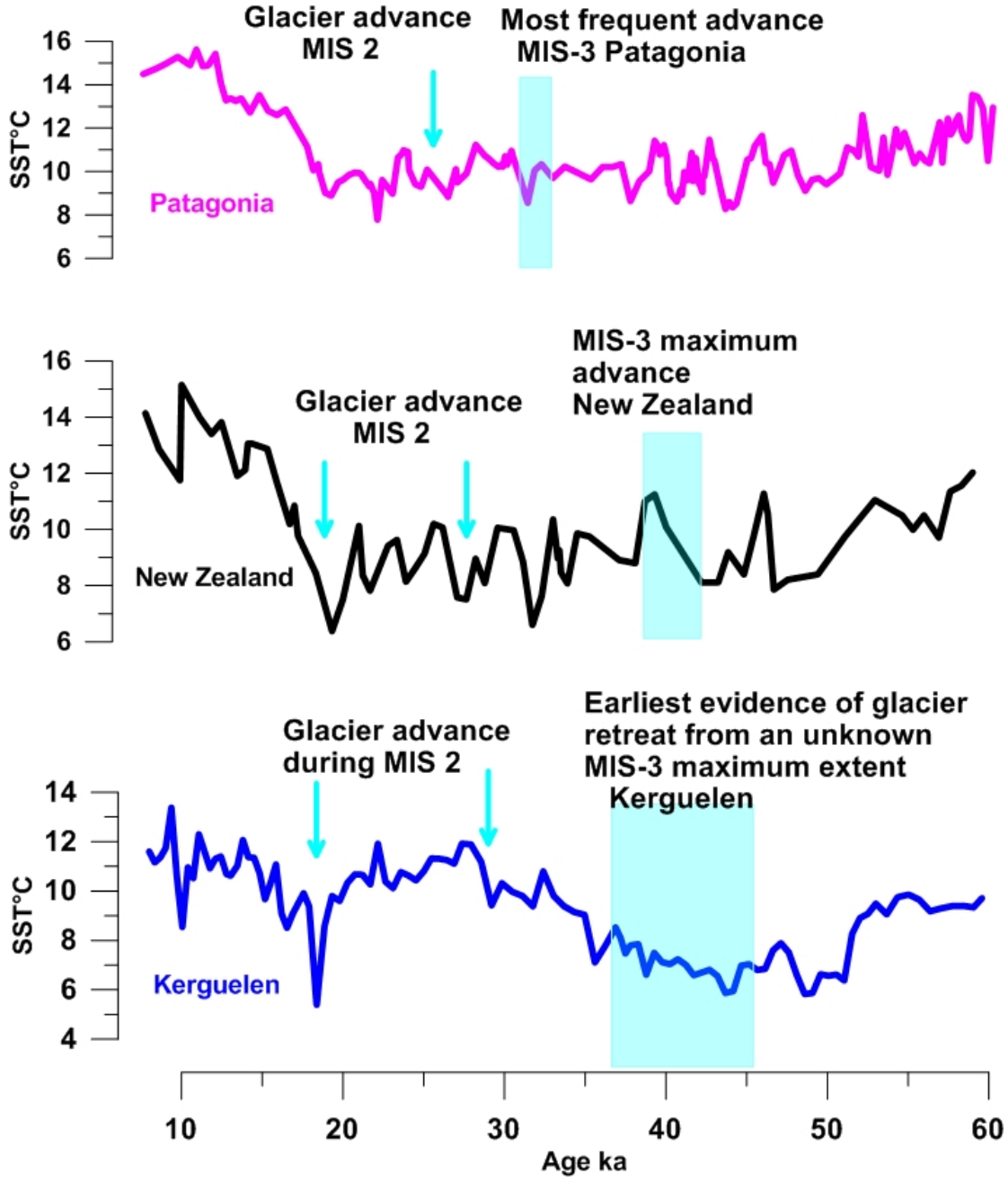

Fig.14. Comparison between sea surface temperature and major glacier extent during MIS-3 and the lLGM in Patagonia (after Darvill et al., 2015; Fogwill et al., 2015), Kerguelen (this study) and New Zealand (after Kelley et al., 2014). Pink curve shows SSTs from the sediment core ODP Site 1233 (41°S) on the east coast of Patagonia, (Kaiser and Lamy, 2010). Black curve shows Sub-Antarctic SSTs from N Chatham Rise MD97-2120 sediment core (45°S)

(Pahnke and Sachs, 2006). Blue curve shows SSTs from Cape Basin 1089/TN057 sediment core (41°S) (Pahnke and Sachs, 2006).

7. Conclusion

Twenty-two cosmogenic ^{36}Cl surface exposure ages were collected from five sites on Kerguelen Archipelago on the eastern slope of the Cook Ice Cap. These samples collected from glacial moraine boulders, erratic boulders and roche moutonnee surfaces made it possible to document changes in glacier extent between 42 ka ago and the late glacial period. The data combined with an earlier record from Kerguelen reveal that glaciers retreated from the maximum extent at ~41 ka ago. From ~41 to ~15 ka, deglaciation generally continued, interrupted by several stagnations or minor culminations, at least at ~28-29 ka and ~24 ka ago. A period of glacier advance occurred prior to ~15-14 ago. These glacier changes at Kerguelen are comparable with glacier fluctuations in New Zealand, but differ from those in Patagonia, where the maximum glacier extent occurred about 13 ka later. The reason of such asynchronous pattern is enigmatic so far, but we hypothesize that it is related to differences in the climate evolution of the Indo-Pacific and Atlantic sectors of Antarctica documented by SSTs from sediment cores and surface air temperature and sea ice extent from proxy ice core records around Antarctica. A transient climatic dipole is created during warming phase of the AIMs with the Atlantic side of Antarctica being warmer than the Indian-Pacific side which may partly be responsible for such different regional climate conditions and by repercussion may explain the reason why Kerguelen glaciers exhibited a different evolution compared to other sub Antarctic regions. However, further investigations of the mechanisms responsible for such asynchronous pattern of climate change are needed to better understand the respective role of external and internal forcings and glacier dynamic.

Acknowledgments

This paper was supported by the French INSU LEFE Glacepreker project and by the IPEV Kesaaco 1048 project. The Cl-36 and Cl measurements were performed at the ASTER AMS national facility (CEREGE, Aix-en-Provence) which is supported by the INSU/CNRS, the ANR through the "Projets thématiques d'excellence" program for the "Equipements d'excellence" ASTER-CEREGE action, and IRD. We are thankful for the compositional analyses at SARM/CRPG.

References

Berthier, E., Le Bris, R., Mabileau, L., Testut, L., Rémy, F., 2009. Ice wastage on the Kerguelen Islands (49°S, 69°E) between 1963 and 2006. J. Geophys. Res. 114, F03005.

Boex, J., Fogwill, C., Harrison, S., Glasser, N.F., Hein, A., Schnabel, C., Xu, S. 2013. Rapid thinning of the late Pleistocene Patagonian Ice Sheet followed migration of the Southern Westerlies. Sci. Rep. 3, 2118; DOI:10.1038/ srep02118.

Buiron, D., Stenni, B., Chappellaz, J., Landais A., Baumgartner, M., Bonazza, M., Capron, E., Frezzotti, M., Kageyama M., Lemieux-Dudon B., Masson-Delmotte V., Parrenin, F.. Schilt, A., Selmo E., Severi, M., Swingedouw, D., Udisti, R. 2012. Regional imprints of millennial variability during the MIS 3 period around Antarctica. Quaternary Science Reviews 48, 99-112.

Clark, P.U., Dyke, A.S., Shakun, J.D., Carlson, A.E., Clark, J., Wohlfarth, B., Mitrovica, J.X., Hosteler, S.W., Mc Cabe, A.M., 2009. The last glacial maximum. Science, 325, 710-714.

Darvill, C.M., Bentley, M.J., Stokes, C.R., Hein, A.S., Rodes, A. 2015. Extensive MIS 3 glaciation in southernmost Patagonia revealed by cosmogenic nuclide dating of outwash sediments. Earth and Planetary Science Letters 429, 157-169.

EPICA Community Members, 2004. Eight glacial cycles from an Antarctic ice core. Nature 429, 623-628.

EPICA Community Members, 2006. One-to-one coupling of glacial climate variability in Greenland and Antarctica. Nature 444, 195-198.

Favier, V., Verfaillie, D., Berthier, E., Menegoz, M., Jomelli, V., Kay, J.E., Ducret, L., Malbéteau, Y., Brunstein, D., Gallée, H., Young-Hyang Park, Y., Rinterknecht, R., 2016. Atmospheric drying as the main driver of dramatic glacier wastage in the southern Indian Ocean. Scientific Reports 6, 32396; doi: 10.1038/srep32396.

Fink D., Vogt S., Hotchkis M., 2000. Cross-sections for ^{36}Cl from Ti at E_p = 35–150 MeV: applications to in-situ exposure dating. Nucl. Instrum. Meth. Phys. Res. Sect. B 172, 861–866.

Frenot, Y., Gloaguen, J.C., Picot, G., Bougère, J., Benjamin, D., 1993. Azorella selago Hook. used to estimate glacier fluctuations and climatic history in the Kerguelen Islands over the last two centuries. Oecologia 95, 140-144.

Frenot, Y., Gloaguen, J.C., Van De Vijver, B., Beyens, L., 1997. Datation de quelques sédiments tourbeux holocènes et oscillations glaciaires aux Iles Kerguelen. Comptes Rendus de l'Académie des Sciences 320, 567-573.

Fletcher, M.S., Moreno, P.I. 2011. Zonally symmetric changes in the strength and positon of the southern westerlies drove atmospheric C02 variations over the past 14 ky. Geology, 39, 419- 422.

Fogwill, C. J., Turney, C.S.M., Hutchinson, D.K., Taschetto, A.S., England, M.H. 2015. Obliquity control on southern hemisphere climate during the Last Glacial. *Sci. Rep.* 5, 11673; doi: 10.1038/srep11673.

579 Hall, K., 1984. Evidence in favour of an extensive ice cover on sub-Antarctic Kerguelen Island during the
580 last glacial. Pal Pal Pal 47, 225-232.
581 Hodgson, D.A., Graham, A.C.G., Roberts, S.J., Bentley, M.J., ÓCofaigh, C., Verleyen, E., Jomelli, V.,
582 Favier, V., Brunstein, D., Verfaillie, D., Colhoun, E.A., Saunders, K., Mackintosh, A., Hall, K., McGlone,
583 M.S., Van der Putten, N., 2014. Terrestrial and marine evidence for the extent and timing of glaciation on
584 the sub-Antarctic islands. Quat. Sci. Rev. 100, 137-158.
585 .http://dx.doi.org/10.1016/j.quascirev.2013.12.001.
586 Ivy-Ochs, S., Synal, H.A., Roth, C., Schaller, M., 2004. Initial results from isotope dilution for Cl and 36Cl
587 measurements at the PSI/ETH Zurich AMS facility. Nuclear Instruments and Methods in Physics Research
588 Section B 223**,** 623- 627.
589 Jomelli, V., Mokadem, F., Schimmelpfennig, I., Chapron, E., Rinterknecht, V., Brunstein, D., Favier, V.,
590 Verfaillie, D., Legentil, C., Michel, E., Swingedouw, D., Jaoen, A., Aster Team 2017. Sub-Antarctic
591 glacier extensions in the Kerguelen region (49°S, Indian Ocean) over the past 24 000 years constrained by
592 ^{36}Cl moraine dating. Quaternary Science Reviews, 162, 128-144.
593 Kaiser, J., Lamy, F. 2010. Links between Patagonian ice Sheet fluctuations and Antarctic dust variability
594 during the last glacial period (MIS 4-2). QSR, 29, 1464-1471.
595 Kelley, S. E., Kaplan, M.R., Schaefer, J.M., Andersen, B.G., Barrell, D.J.A., Putnam, A.E., Denton, G.H.,
596 Schwartz, R., Finkel, R.C., Doughty, A.M. 2014. High-precision 10Be chronology of moraines in the
597 Southern Alps indicates synchronous cooling in Antarctica and New Zealand 42,000 years ago. *Earth and*
598 *Planetary Science Letters* **405,** 194–206, doi:http://dx.doi.org/10.1016/j. epsl.2014.07.031.
599 Lamy, F., Kilian, R., Arz, H.W., Francois, J.P., Kaiser, J., Prange, M., Steinke, T. 2010. Holocene changes in
600 the position and intensity of the southern westerly wind belt. Nature Geoscience 3, 695–699.
601 Landais, A., Masson-Delmotte, V., Stenni, B., Selmo, E., Roche, D., Jouzel, J., Lambert, F., Guillevic, M., Bazin, L.,
602 Arzel, O., Vinther, B., Gkinis, V., Popp, T. (2015). A review of the bipolar see–saw from synchronized and high
603 resolution ice core water stable isotope records from Greenland and East Antarctica, Quaternary Science Reviews,
604 114, 18-32
605 Merchel, S., Bremser W., Alfimov V., Arnold M., Aumaître G. , Benedetti L., Bourlès D. L.,Caffee M.
606 Fifield L. K., Finkel R. C., Freeman S. P. H. T., Martschini M., Matsushi Y., Rood D. H., Sasa K., Steier
607 P., Takahashi T.,Tamari M. , Tims S. G. , Tosaki Y., Wilcken K. M., Xu S. (2011). Ultra-trace analysis
608 of 36Cl by accelerator mass spectrometry: an interlaboratory study. Anal Bioanal Chem DOI
609 10.1007/s00216-011-4979-2
610 Otto-Bliesner, B. L., E. Brady, G. Clauzet, R. Tomas, S. Levis, and Z. Kothavala, 2006a: Last glacial
611 maximum and holocene climate in CCSM. J. Climate, 19, 2526–2544.

612 Pahnke, K., Sachs, J.P. 2006. Sea surface temperatures of southern midlatitudes 0-160 kyr BP.
613 Paleoceanography, 21, PA2004, doi:10.1029/2005PA001191.
614 Parrenin, F., Masson-Delmotte, V., Köhler, P., Raynaud, D., Paillard, D., Schwander, J., Barbante, C.,
615 Landais, Wegner, A., Jouzel, J. 2013. Synchronous Change of Atmospheric CO2 and Antarctic
616 temperature during the last deglacial warming. Science, 339, 1060-1063.
617 Phillips, F.M., Stone, W.D., Fabryka-Martin, J.T., 2001. An improved approach to calculating low-energy
618 cosmic-ray neutron fluxes near the land/atmosphere interface. Chem. Geol. 175, 689–701.
619 Poggi, A. 1977. Heat Balance in ablation area of Ampere Glacier (Kerguelen Islands). J. Appl. Meteorol.,
620 16, 48-55, doi:10.1175/1520 0450(1977)016<0048:HBITAA>2.0.CO;2.
621 Putnam, A Schaefer, J., Denton, G.H., Barrel, D.J.A., Anderson, R.F., Koffman, T.N.B., Rowan, A.V.,
622 Finkel, R.C., Rood, D.H., Schwartz, R., Vandergoes, M.J., Plummer, M.A., Brocklehurst, S.H., Kelley,
623 S.E., Ladig, K.L. 2013. Warming and glacier recession in the Rakaia valley, Southern Alps of New
624 Zealand, during Heinrich Stadial 1. EPSL, 382, 98-110.
625 Rind, D., J., Lerner, J., C. McLinden, C., Perlwitz1, J. 2009. An analysis of the Stratospheric ozone during
626 the Last Glacial Maximum. GRL 36, L09712, doi:10.1029/2009GL037617,
627 Rojas, M., Moreno, P., Kageyama, M., Crucifix, M., Hewitt, C., Abe-Ouchi, A., Ohgaito, R., Brady, E.C.,
628 Hope, P. 2009. The Southern Westerlies during the last glacial maximum in PMIP2 simulations. Clim
629 Dyn, 32, 525–548.
630 Schaefer, J., Putnam A.E., Denton, G.H., Kaplan, M.R., Birkel, S., Doughty, A.M., Kelley, S., Barrel,
631 D.J.A., Finkel, R.C., Winckler, G., Anderson, R.F., Ninneman, U.S., Barker, S., Swartz R., Andersen B.,
632 G., Schluechter, C. 2015. The Southern Glacial maximim 65,000 years ago and ist unfinished termination.
633 QSR. 114, 52-60.
634 Schimmelpfennig, I., Benedetti, L., Finkel, R., Pik, R., Blard, P.-H., Bourlès, D., Burnard, P., and Williams,
635 A., 2009. Sources of in-situ 36 Cl in basaltic rocks. Implications for calibration of production rates:
636 Quaternary Geochronology 6, 441-461.
637 Schimmelpfennig, I., Benedetti, L., Garreta, V., Pik, R., Blard, P.-H., Burnard, P., Bourles, D., Finkel, R.,
638 Ammon, K., Dunai, T., 2011. Calibration of cosmogenic 36 Cl production rates from Ca and K spallation
639 in lava flows from Mt. Etna (38 N, Italy) and Payun Matru (36 S, Argentina): Geochimica et
640 Cosmochimica Acta 75, 2611-2632
641 Schimmelpfennig, I. Schaefer, J., Putnam, A., Koffman, T., Benedetti, L., Ivy-Ochs, S., ASTER Team,
642 Schlüchter, C., 2014. ^{36}Cl production rate from K-spallation in the European Alps (Chironico landslide,
643 Switzerland). Journal of Quaternary Science 29, 407–413.
644 Sharma, P., Kubik, P.W., Fehn, U., Gove, H.E., Nishiizumi, K., Elmore, D., 1990. Development of ^{36}Cl
645 standards for AMS. Nuclear Instruments and Methods in Physics Research Section B 52, 410-415.

Sime, C.C., Kohfeld, K.E., Le Quéré, C., Wolff, E.W., de Boer, A.M., Graham, R.M., Bopp, L. (2013). Southern Hemisphere westerly wind changes during the Last Glacial Maximum: model-data comparison. Quaternary Science Reviews 64, 104-120.

Stenni, D., Masson-Delmotte, V., Selmo, E., Oerter, H., Meyer, H., Rothlisberger, R. Jouzel, J.,Cattani, O., Falourd, S. , Fischer, H., Hoffmann, G. Iacumin, P. Johnsen, S.J., Minster, B., Udisti R. 2010. The deuterium excess records of EPICA Dome C and Dronning Maud Land ice cores (East Antarctica). Quaternary Science Reviews 29, 146–159.

Stenni, B., Buiron, D., Frezzotti, M., Albani, S., Barbante, C., Bard, E., Barnola, J. M., Baroni M., Baumgartner, M., Bonazza, M., Capron, E., Castellano, E., Chappellaz, J., Delmonte, B., Falourd, S.,Genoni, L., Iacumin, P., Jouzel, J., Kipfstuhl, S., Landais, A., Lemieux-Dudon, B., Maggi, V., Masson-Delmotte, V., Mazzola, C., Minster, B., Montagnat, M., Mulvaney, R., Narcisi, B., Oerter, H., Parrenin, F., Petit, J. R., Ritz, C., Scarchilli, C., Schilt, A., Schüpbach, S., Schwander, J., Selmo, E., Severi, M., Stocker, T. F., Udisti, R. 2011. Expression of the bipolar see-saw in Antarctic climate records during the last deglaciation. Nature Geoscience. 4, 46-49.

Stone, J.O., 2000. Air pressure and cosmogenic isotope production. Journal of Geophysical Research 105, 23753-23759.

Stone J.O., Fifield, K., Vasconcelos, P., 2005. Terrestrial chlorine-36 production from spallation of iron. Abstract of 10th International Conference on Accelerator Mass Spectrometry. September 5-10, 2005, Berkeley, USA. http://llnl.confex.com/llnl/ams10/techprogram/P1397.HTM.

Thompson, D.W.L., Wallace, J.M., 2000. Annular modes in the extratropical circulation. Part 1: Month to month variability. J. Climate, 13, 1000-1016.

Thompson, D. W. J., Solomon, S., Kushner, P.J., England, M.H., Grise, K.M., Karoly, D.J., 2011. Signatures of the Antarctic ozone hole in Southern Hemisphere surface climate change. Nature Geoscience 4, 741-749.

Vallon, M. 1977a. Bilan de masse et fuctuations recentes du Glacier Ampere (Iles Kerguelen, TAAF). Zeitschrift fur Gletscherkunde und Glazialgeologie, 13, 55-85.

Vallon, M. 1977b. Topographie sous glaciaire du Glacier Ampere (Iles Kerguelen, TAAF). Zeitschrift fur Gletscherkunde und Glazialgeologie, 13, 37-55.

Vallon, M. 1987. Glaciologie a Kerguelen, Proceedings of the Colloque C.N.F.R.A. sur la Recherche Francaises dans les Terres Australes, Strasbourg, 11-17 September 1987.

Verfaillie, D., Favier, V., Dumont, D. Jomelli, V., Gilbert, A., D. Brunstein, D., H. Gallée, H. Frenot Y., 2015. Recent glacier decline in the Kerguelen Islands (49°S, 69°E) derived from modeling, field observations, and satellite data. JGR 120, 637-654.

679 Vimeux, F., Cuffey, K. M., Jouzel, J. 2002. New insights into Southern Hemisphere temperature changes
680 from Vostok ice cores using deuterium excess correction, Earth Planet. Sci. Lett., 203, 829–843,
681 doi:10.1016/S0012-821X(02)00950-0.
682 WAIS Divide Project Members 2015. Precise interpolar phasing of abrupt climate change during the last
683 ice age. Nature 520, 661-665.
684 Watanabe, O., Jouzel, J., Johnsen, S., Parrenin, F., Shoji, H., Yoshida, N., 2003. Homogeneous climate
685 variability across East Antarctica over the past three glacial cycles. Nature 422, 509– 512.
686
687 **Author Contributions:** V.J., D.B., D.V., V.R., C.L. and V.F. conducted the field work on the Island; F.M. produced
688 the cosmogenic data, ASTER Team performed AMS measurements; I.S., V.M., V.R. and V.J. interpreted the
689 cosmogenic ages; A.L. V.J. interpreted the ice core signal; V.J. and I.S. prepared figures and V.J., I.S., V.R., V.F.,
690 D.V. and A.L. contributed to writing the paper.
691
692
693
694
695
696
697
698
699
700
701